# Real-time detection of sleep apnea and hypopnea syndrome by individual-based model

**Hui Yu [1], Chenyang Deng [2], Jinglai Sun [3], Yanjin Chen [4] and Yuzhen Cao [5*]**

[1] Department of Biomedical Engineering, Tianjin University, Tianjin, China
[2] Department of Biomedical Engineering, Tianjin University, Tianjin, China
[3] Department of Biomedical Engineering, Tianjin University, Tianjin, China
[4] Tianjin Hospital of ITCWM Nankai Hospital, Tianjin, China
[5] Department of Biomedical Engineering, Tianjin University, Tianjin, China, Tel: 086-022-27406546, E-mail: yzcao@tju.edu.cn

## Abstract:

Sleep apnea and hypopnea syndrome (SAHS) affects the quality of people's life and may lead to various kinds of diseases. In this paper, an individual-based method is proposed for real-time detection of SAHS using the features extracted from both nasal flow (NF) and saturation of peripheral oxygen ($SpO_2$). An overlapping window was utilized to help segment the original signals and locate the start and end time of SAHS. Nine time-frequency features were extracted from each segment and fed into a support vector machine (SVM) for a fivefold cross validation. Individual-based model was trained and finally real-time detection of SAHS with one-second resolution was achieved with a sensitivity (Sen) of 89.6% and a specificity (Spe) of 91.7% in average. It is shown in the experimental results that this method has a more generalization ability within different people compared with previous studies and can be a strong candidate for the real-time detection of SAHS clinically.

**Key words:** Sleep apnea and hypopnea syndrome, Real-time detection, Individual-based model, SVM, Nasal flow, $SpO_2$

## 1. Introduction:

Sleep apnea and hypopnea syndrome (SAHS) is a highly prevalent sleep disease which is estimated to affect 2-4% of the middle-aged population [1]. It may cause sleepiness and fatigue during daytime and lead to more road traffic accidents [2]. Even worse, SAHS is also related to some cardiovascular diseases though not definitively [2].

Polysomnogram (PSG) is the gold standard for SAHS detection. However, it is expensive, time consuming and labor intensive. In order to find a substitute for PSG, some research groups[3-5] have proposed several automatic methods to evaluate the severity of SAHS. However, these researches rely on a delayed diagnosis based on the overnight signals. On the other side, there are also some methods developed to detect SAHS in real time. Bsoul, M et al. [6] employed SVM to detect apnea based on the features from one-minute ECG epoch using the Apnea-ECG database [7]. Baile Xie and Hlaing Minn [8] applied classifier combination in the real-time SAHS detection based on the features extracted both from ECG and $SpO_2$. H. D. Nguyen et al. [9] introduced an online sleep apnea detection method based on heart rate complexity using a fusion of SVM and neural network (NN). Most recently Hyoki Lee et al. [10] developed a rule-based algorithm for automatic real-time detection of SAHS using a nasal pressure signal and achieve a sensitivity of 86.4%.

Among these studies, only Bsoul, M et al. have run an individual-based experiment. The rest studies mainly put the focus on the features extracted for training and different algorithms for classification while ignore the generalization ability of the method for different groups of people. Furthermore, all studies above except Hyoki Lee et al. are only able to achieve a time resolution of one-minute instead of detecting the start and duration of SAHS. In view of that, this paper aims to propose a method that can be applied to different groups of people for real-time detection of SAHS with a high time resolution. The flow chart of the process of this study is shown in Fig. 1.

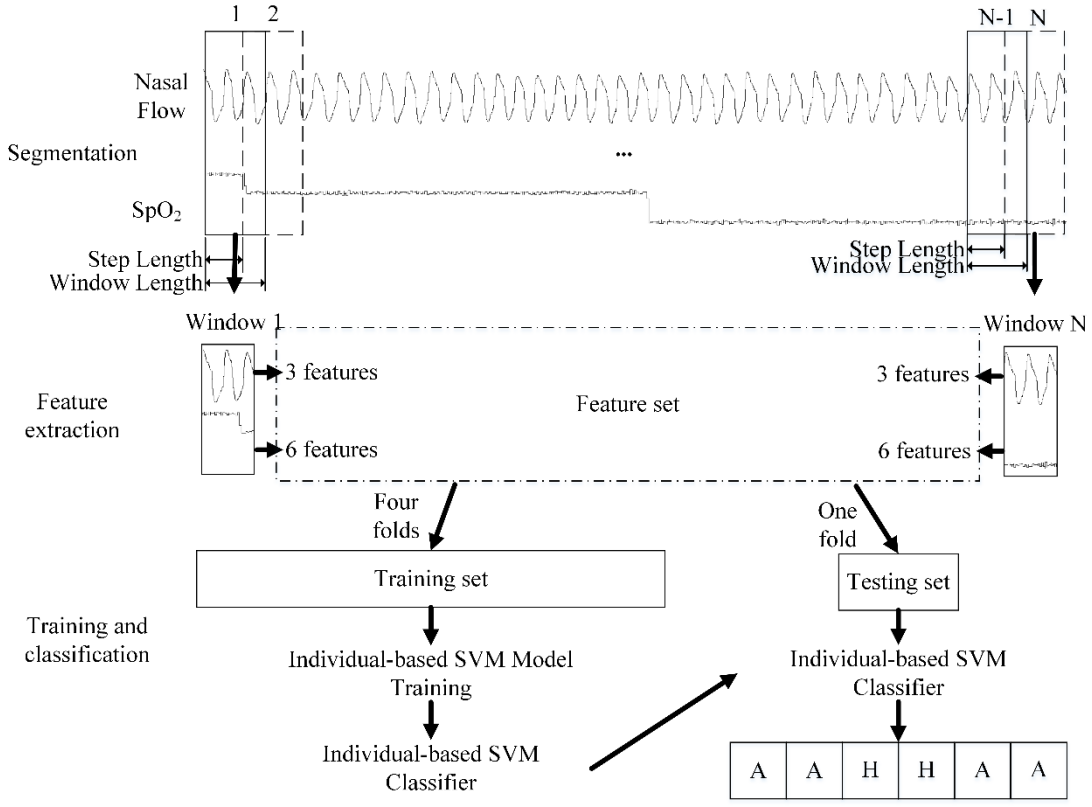


**Fig. 1** The flow chart of the process of this study

Since $SpO_2$ and NF are the two straightforward signals to score SAHS according to the 2012 AASM criteria [11], both signals were adopted for SAHS detection in this paper. Firstly, we utilized an overlapping window to slide over the original signals for segmentation. As a result, both signals were divided into a series of segments with fixed width and interval. Form each segment we extracted nine features for the following training and classification. A SVM model was trained for every subject and the performance of it was evaluated using a fivefold cross validation. Besides, the effects of different overlapping windows and feature sets were tested in the experimentation. Finally, a real-time detection of SAHS with a sensitivity of 89.6% and a specificity of 91.7% in average was achieved.

This paper is divided into five sections. The first section contains the introduction. The second section describes the database and the methods adopted in our experiment. The third section shows the classification results of different parameters and training strategies. The forth section discusses the influence of different parameters and the comparison with other research groups. The last section concludes this paper.

## 2. Materials and Methods

### 2.1. Database

ST. Vincent's University Hospital/University College Dublin Sleep Apnea Database [12] is used throughout this study. This database is available on Physionet [13]. Twenty-five full overnight polysomnograms with detailed start time and duration of every SAHS event are included in this database. The following experiments ran on MATLAB 2013b using a computer with Intel core i5-7600K CPU. All graphics were performed with Excel 2016.

The $SpO_2$ signal is sampled from a finger pulse oximeter while the NF signal is from a thermistor. The sample frequencies are both 8Hz. All subjects in this database are above eighteen years of age with no known cardiovascular diseases interfere with heart rate [12]. The details of the subjects are shown in the Table 1.

**Table 1** The details of the subjects in ST. Vincent's University Hospital/University College Dublin Sleep Apnea Database

| Number of Subjects | Gender Distribution | Age Range (Years) | Study Duration Range (Hours) | SAHS Duration Range (Hours) | Normal Duration Range (Hours) |
|---|---|---|---|---|---|
| 25 | 4F&21M | [28 68] | [5.9 7.7] | [0.1 2.8] | [3.1 7.4] |

Due to the loss of the NF signal in subject 3&9 in the dataset, only the rest twenty-three subjects were taken into study in the following work. Besides $SpO_2$ in some periods falls lower than 50% which may be caused by the loose contact between skin and sensor. As a result, these periods were also not taken into study. It has been found that the imbalance in the species of training patterns always has a great effect on the training success [14]. However, the SAHS duration is less than a quarter of the normal duration in most subjects in the dataset thus making it difficult for fully training the individual-based models. Therefore, we applied an overlapping window to segment the original signals.

### 2.2. Signal preprocessing

The overlapping window is determined by the window length $L_w$ and the step length $L_s$ and abbreviated as $W_{Lw,Ls}$ in the rest of paper. Both signals were divided into a series of segments with it. As a result, the length of each segment was $L_w$ seconds meanwhile there was a $L_s$-second interval between the two consecutive segments. Besides, the original annotation files were transformed into label files with either

positive (1) or negative (0). The segment with less than three consecutive seconds of SAHS was labeled negative. Otherwise, it was labeled positive. The number of segments obtained per subject in average using windows with different $L_s$ is shown in Fig. 2.

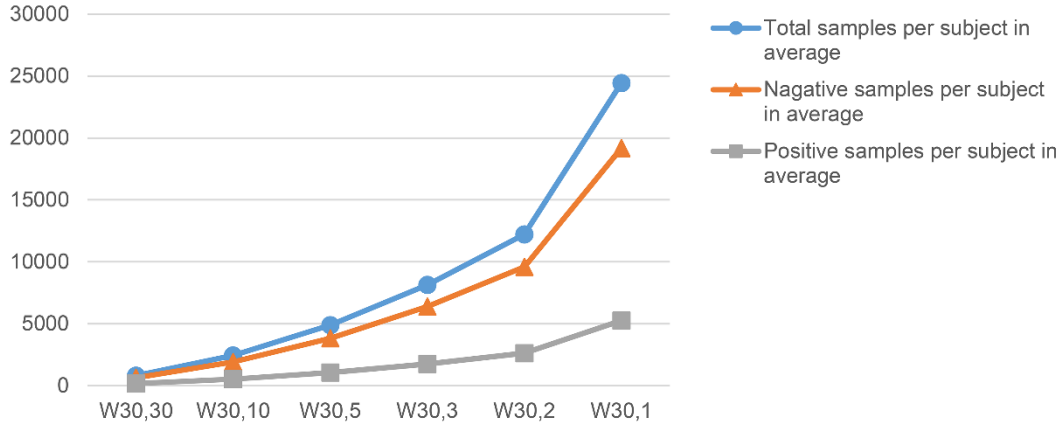


**Fig. 2** The number of samples per subject in average we obtain with different $L_s$

It is illustrated that only less than one thousand samples are obtained per subject in average with a no overlapping window. While as the $L_s$ sets shorter, several times more samples can be received thus making it possible to get the individual-based model fully trained.

### 2.3. Feature extraction

From the perspective of reducing the computation, some typical nonlinear features used before such as Lempel-Ziv complexity [8,3,15,16] and approximate entropy [8,3,15,16] were not taken into study. On the contrary, we adopted some easily calculated features.

There is always significant fluctuations in the $SpO_2$ recordings from patients affected by SAHS because of the desaturation events [17]. Therefore, the standard deviation was calculated as an approximate measure of the fluctuation in each $SpO_2$ segment and denoted as *Spstd*. Secondly a regression line was fitted for every $SpO_2$ segment [8] in a least squares sense then the absolute slope (*Spmu*) and bias (*Spbia*) of the regression line were calculated to show the tendency of each segment. Besides, oxygen saturation in normal subjects tends to stay constant around 96%, while in the SAHS-positive patients significant changes can be found due to the recurrent apnea events [18]. Therefore, the accumulative time spent below 93% and the mean value (*Spl93, Splm*) of each segment was calculated to represent the significant changes between positive and negative segments. Additionally, the commonly used saturation variability index (*Delta index*) [19,8,20] was also adopted in this study. People normal respiratory rate is twelve per minute. As a result, the sum value of every ten-second $SpO_2$ interval was first calculated and the Delta index was derived as the differences between the two sum values of successive intervals. The six features constituted the $SpO_2$ feature set (SPFS).

Furthermore, the variability and irregularity of NF may be modified by the complete or partial collapse of the upper airway in SAHS-positive patients [3]. Based on that, the tidal volume was firstly calculated in every ten-second interval and the changes in tidal volume of the two consecutive intervals (*Fdif*) were measured to show the variability in NF. Besides, the main frequency energy of NF signal was calculated and denoted as *Fmp*. In addition, a spectral band of interest was defined between 0 Hz and 0.5 Hz corresponding to the people respiratory rate. And the standard deviation (*Fsd*) of FFT in this band was calculated to show the irregularity of the NF segment. The three features constituted the NF feature set (NFFS) and totally nine features were extracted from each segment. The details of each feature are

shown in Table 2.

**Table 2** Detailed description of each feature

| | Feature Name | Description |
|---|---|---|
| $SpO_2$ Feature Set (SPFS) | *Spstd* | The Standard deviation of each $SpO_2$ segment |
| | *Spmu* | The absolute slope of the regression line fitted for each $SpO_2$ segment |
| | *Spbia* | The bias of the regression line fitted for each $SpO_2$ segment |
| | *Spl93* | The accumulative time that $SpO_2$ stays lower than 93 |
| | *Splm* | The accumulative time that $SpO_2$ stays lower than the mean value of each $SpO_2$ segment |
| | *Delta index* | The differences between the two sum values of successive ten-second interval |
| NF Feature Set (NFFS) | *Fmp* | The proportion of main frequency energy to total energy |
| | *Fdif* | The differences between the two tidal volumes of successive ten-second interval |
| | *Fsd* | The standard deviation of FFT in the interest spectral band |

### 2.4. Training and classification

SVM has been developed by Vapnik [21] and has a high generalization ability for two-group classification through mapping original features into a very high-dimension feature space.

Here the SVM model contains four kinds of kernels with different kernel parameters. In addition to that, the penalty factor C determines the level of soft margin for the model. Gaussian radial basis functions (RBF) was utilized in this study because of its high numerical and geometrical efficiency for classifying nonlinear data. The following experiments were conducted with the radius of RBF kernel and the penalty factor C both set to one. Features were normalized before fed into the SVM model. It should be noted that for each subject there would be one SVM model trained and totally twenty-three models were trained in the end. Furthermore, every SVM model was trained using a fivefold cross validation and the experiment result was averaged over five folds in order to avoid the risk of overfitting implicitly due to the sample redundancy caused by the utilization of overlapping window. To achieve that, the feature sets of each subject were randomly divided into five folds. Each time onefold would be chosen to be the testing group while the rest folds were used for training group.

Firstly, individual-based model was trained with the full feature set extracted from a thirty seconds window with different $L_s$. In next experiment, individual-based model was trained using the full feature set extracted from a window with different $L_w$. Then individual-based model was trained using SPFS and NFFS separately. Finally, non-individual-based model was trained using the same features in the same way as the individual-based model.

## 3. Results

A sensitivity-specificity plot was used to evaluate the performance of the model. Sensitivity, specificity and accuracy (Acc) are defined as the equation (1), (2) and (3) show.

$$sensitivity = 100 \times \frac{TP}{TP+FN} \tag{1}$$

$$specificity = 100 \times \frac{TN}{TN+FP} \tag{2}$$

$$accuracy = 100 \times \frac{(TP+TN)}{(TP+FP+TN+FN)} \quad (3)$$

Here *TP* refers to the number of true positives while *TN* refers to the number of true negatives. On the contrary, *FP* and *FN* represent the number of false positives and false negatives respectively. Sensitivity and specificity represent the ability to identify the positives and negatives. The result of every subject was pointed in the sensitivity-specificity plot. And the point on the top right represents a better performance.

### 3.1. Classification results of different $L_s$

The classification results using the full feature set extracted from the thirty seconds window with different $L_s$ are firstly shown in Fig. 3.

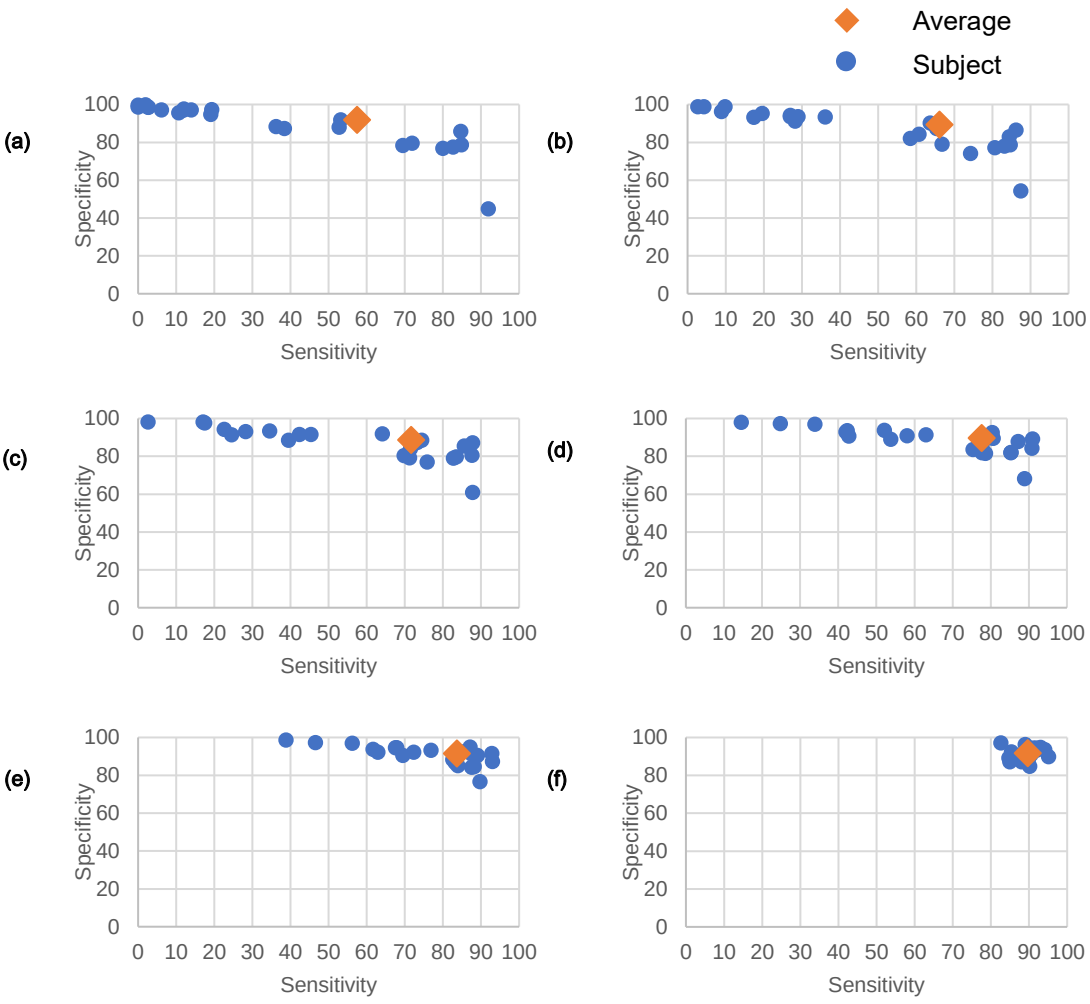


**Fig. 3** **a** The classification results of $W_{30,30}$. **b** The classification results of $W_{30,10}$. **c** The classification results of $W_{30,5}$. **d** The classification results of $W_{30,3}$. **e** The classification results of $W_{30,2}$. **f** The classification results of $W_{30,1}$

The SVM classifier only reached a sensitivity of 57.5% in average using a no overlapping window (see Fig. 3(a)). When the $L_s$ was set to ten seconds, the sensitivity increased to 66.1% in average (see Fig. 3(b)). However, the SVM classifier reached a specificity of over 90.0% but a sensitivity lower than 40.0%

in some subjects just as the points in the top left show. Besides, there was also a subject with a sensitivity of 87.5% but a specificity of 54.4%. This was a result of the model not being fully trained because of the lack of training samples (see Fig. 2). However, the SVM classifier performed more stably among different subjects and provided a better performance as the $L_s$ set shorter (see Fig. 3(c), (d) and (e)). When the $L_s$ was set to one second, the SVM classifier reached a sensitivity of 89.6% and a specificity of 91.7% in average (see Fig. 3(f)). Moreover, the SVM classifier had a strong generalization ability among different subjects. As a result, the $L_s$ was set to one second and the influence of $L_w$ was taken into analysis in the following study.

### 3.2. Classification results of different $L_w$

The classification results using the full feature set extracted from the window with different $L_w$ are shown in Fig. 4.

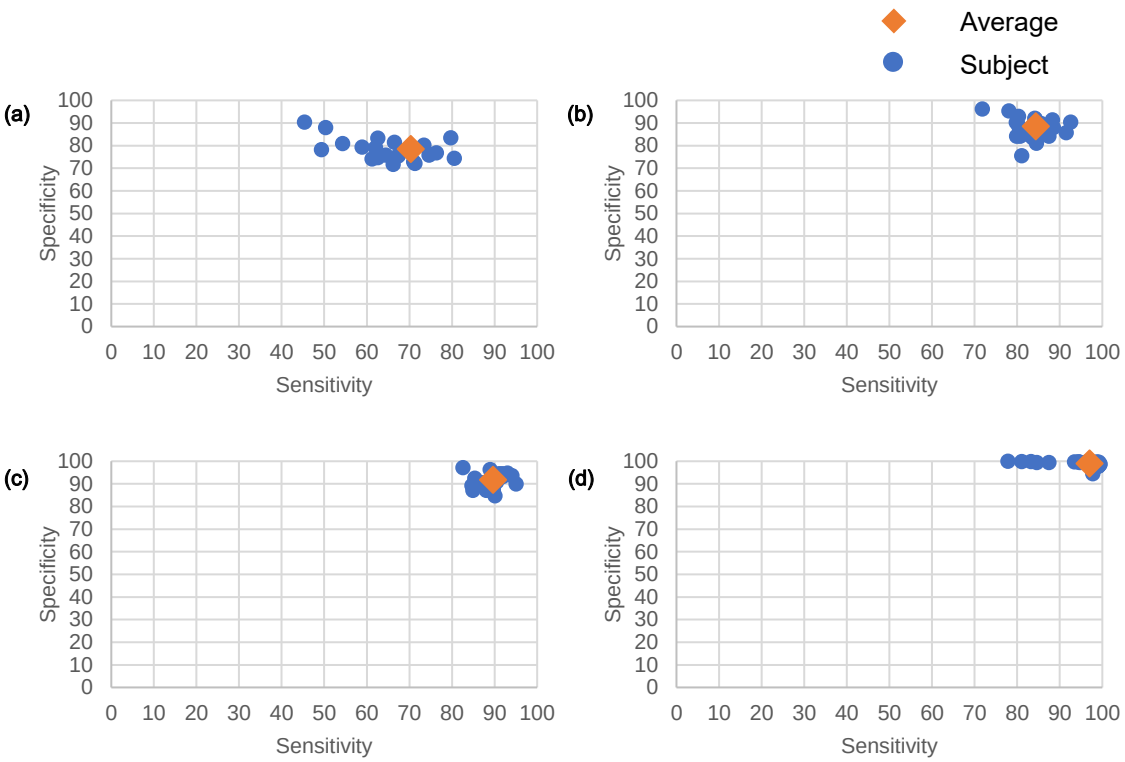


**Fig. 4** **a** The classification results of $W_{10,1}$. **b** The classification results of $W_{20,1}$. **c** The classification results of $W_{30,1}$. **d** The classification results of $W_{60,1}$

The SVM classifier reached a sensitivity of 70.3% in average with $W_{10,1}$. However, there is a significant variance among different subjects (see Fig. 4(a)). With the $L_w$ set longer than ten seconds, the sensitivity of over 84.4% and the specificity of over 88.6% in average were reached (see Fig. 4(b), (c) and (d)). Meanwhile the SVM classifier performed stably among different subjects.

### 3.3. Classification results using SPFS and NFFS separately

The classification results using SPFS, NFFS and the full feature set respectively are tabulated in Table 3.

**Table 3** The classification results using SPFS, NFFS and the full feature set respectively extracted

from $W_{30,1}$

| Feature set | Acc (%) | Sen (%) | Spe (%) |
|---|---|---|---|
| SPFS | 82.8 | 82.3 | 82.9 |
| NFFS | 74.7 | 77.4 | 73.9 |
| The full feature set | 91.3 | 89.6 | 91.7 |

Table 3 shows that there are different degrees of decline in all three measures when we use either SPFS or NFFS alone. When we switched from the full feature set to SPFS, all three measures decreased by around ten percent. As for NFFS, the decrease was heavier. Which indicates that the SPFS and NFFS can complement each other in the real-time detection and the combination of them provides an improvement in the classification results.

### 3.4. Classification results of non-individual-based model

The comparison between individual-based and non-individual-based model is shown in Table 4.

**Table 4** The classification results of individual-based model and non-individual-based model in average

| Window | Model type | Acc (%) | Sen (%) | Spe (%) |
|---|---|---|---|---|
| $W_{20,1}$ | individual-based | 87.8 | 84.4 | 88.6 |
| | non-individual-based | 86.0 | 75.7 | 87.2 |
| $W_{30,1}$ | individual-based | 91.3 | 89.6 | 91.7 |
| | non-individual-based | 86.2 | 75.7 | 87.4 |
| $W_{60,1}$ | individual-based | 98.4 | 97.0 | 98.9 |
| | non-individual-based | 83.1 | 75.9 | 84.0 |

For the case of non-individual-based model, there were decreases in all three measures especially in the sensitivity compared to individual-based model. Taking individual differences into consideration, different people may differ in the inspiratory time and expiratory time. Besides, there are also differences in the amplitude and frequency in breath among different people. The non-individual-based model is not able to adapt itself to the individual differences thus does not have a strong generalization ability like the individual-based model.

## 4. Discussion

### 4.1. The influence of $L_s$

On one hand $L_s$ determines the number of samples for training. On the other hand, it represents the time resolution of the detection. Fig. 2 shows that when we set $L_s$ to one second, several times more training samples are obtained though the imbalance between positive and negative still exists, there are over five thousand positive samples for training. Thus, the influence of the imbalance can be minimized. Fig. 3 illustrates that the individual-based model provides a good performance with the $L_s$ set to one second. As a result, we are able to locate the start and end time of SAHS in second with it.

### 4.2. The influence of $L_w$

$L_w$ represents the data length required for feature extraction and detection. Fig. 4 shows that the classifier is able to provide a good performance with the $L_w$ set to longer than ten seconds. It is thought that with

a longer window, there would be more data to be processed thus more time would be required for detection. Here the processing time using different windows is tabulated in Table 5.

**Table 5** Comparison with different $L_w$

| Window | Acc (%) | Sen (%) | Spe (%) | Processing Time (10000 Samples) |
|---|---|---|---|---|
| $W_{10,1}$ | 77.4 | 70.4 | 78.5 | 7.12 |
| $W_{20,1}$ | 87.8 | 84.4 | 88.6 | 6.75 |
| $W_{30,1}$ | 91.3 | 89.6 | 91.7 | 6.58 |
| $W_{60,1}$ | 98.4 | 97.0 | 98.9 | 7.57 |

Around seven seconds would be spent on processing ten thousand samples whatever window we utilized (see Table 5). It should be noted that the processing time not only relies on the data length required for feature extraction and detection, but also affected by the complexity of SVM model. However, the complexity of SVM model can be significantly decreased with the individual-based method and the small amount of features we extracted. Hence the response time of this method is expected to meet the demand in real-time detection.

### 4.3. Comparison with other related work

As mentioned in the introduction, several methods have been developed to detect SAHS on an epoch basis [6,8-10]. A summary of these methods is presented in Table 6.

**Table 6** Comparison with other related works

| Methods | Acc (%) | Sen (%) | Spe (%) | Resolution | Features | Database |
|---|---|---|---|---|---|---|
| SVM with RBF kernel function[6] | 89.3 | 95.1 | 85.9 | 1min | 111ECG features | Apnea-ECG database |
| Bagging.ERPTree + AdaBoost + decision Table[8] | 81.0 | 83.6 | 80.1 | 1min | 8ECG features 31$SpO_2$ features | UCD database |
| Soft decision fusion from SVM and NN[9] | 85.2 | 86.4 | 83.5 | 1min | 72ECG features | Apnea-ECG database |
| Detection based on different thresholds[10] | Nan | 88.5 | Nan | Nan | Nasal pressure features | Clinical data |
| SVM with RBF kernel function (this paper) | 91.7 | 91.3 | 89.6 | 1s | 8$SpO_2$ features 3NF features | UCD database |

Compared to the studies before, it is exhibited in Table 6 that our SHAS detection method provides a good performance compared with other approaches. Individual-based model for different people, high time resolution and the combination of $SpO_2$ and NF signals are three bright points in this paper. Firstly, individual-based model was trained by a sufficient number of samples obtained through the utilization of the overlapping window and was adaptive to different people compared to the non-individual-based model. Secondly, one-second resolution was achieved without degrading the classification results (see Fig. 3) which can help us locate the start and end time of SAHS. Thirdly, the nasal flow and $SpO_2$ signals are able to complement each other. Therefore, using the combination of $SpO_2$ and NF is able to provide a better performance than using them alone just as Table 3 shows.

On the other hand, several limitations remain in this study. Though twenty-three subjects are

included, still larger populations are expected to test the generalization ability of this method. Besides, this study is conducted offline while the redundancy caused by the overlapping window may lead to the overfitting of the individual-based model though a fivefold cross validation is included in this paper. We are looking forward to conducting an online test in the future.

## 5. Conclusion

Real-time SAHS detection by training individual-based model has been studied in this paper using totally nine features extracted from $SpO_2$ and NF signals. The influence of the overlapping window and the feature sets are tested in the experimentation. The experimental results indicate that the performance of our proposed method is good and the complexity of the method is decreased by the small amount of features we extract and the individual-based model trained for every subject. Therefore, this method is considered to have a more generalization ability for different groups of people and expected to be a strong candidate for the real-time SAHS detection clinically.

## Acknowledgements

We thank the sleep apnea database provided by St. Vincent's University Hospital Sleep Disorders Clinic on https://www.physionet.org/physiobank/database/ucddb/ and the Medical guidance provided by the Tianjin Hospital of ITCWM Nankai Hospital.

**References:**


1. Young, T., Palta, M., Dempsey, J., Skatrud, J., Weber, S., & Badr, S. (1993). The occurrence of sleep-disordered breathing among middle-aged adults. [; Research Support, U.S. Gov't, P.H.S.]. *The New England journal of medicine, 328*(17), 1230-1235, doi:10.1056/nejm199304293281704.
2. Jordan, A. S., McSharry, D. G., & Malhotra, A. (2014). Adult obstructive sleep apnoea. [Article]. *Lancet, 383*(9918), 736-747, doi:10.1016/s0140-6736(13)60734-5.
3. Gutierrez-Tobal, G. C., Alvarez, D., del Campo, F., & Hornero, R. (2016). Utility of AdaBoost to Detect Sleep Apnea-Hypopnea Syndrome From Single-Channel Airflow. *Ieee Transactions on Biomedical Engineering, 63*(3), 636-646, doi:10.1109/tbme.2015.2467188.
4. Chen, L., Zhang, X., & Song, C. (2015). An Automatic Screening Approach for Obstructive Sleep Apnea Diagnosis Based on Single-Lead Electrocardiogram. *IEEE Transactions on Automation Science and Engineering, 12*(1), 106-115, doi:10.1109/TASE.2014.2345667.
5. Sharma, H., & Sharma, K. K. (2016). An algorithm for sleep apnea detection from single-lead ECG using Hermite basis functions. *Computers in Biology and Medicine, 77*, 116-124, doi:https://doi.org/10.1016/j.compbiomed.2016.08.012.
6. Bsoul, M., Minn, H., & Tamil, L. (2011). Apnea MedAssist: Real-time Sleep Apnea Monitor Using Single-Lead ECG. [Article]. *Ieee Transactions on Information Technology in Biomedicine, 15*(3), 416-427, doi:10.1109/titb.2010.2087386.
7. Penzel, T., Moody, G. B., Mark, R. G., Goldberger, A. L., Peter, J. H., Ieee, et al. (2000). The apnea-ECG database. In *Computers in Cardiology 2000, Vol 27* (Vol. 27, pp. 255-258, Computers in Cardiology Series). New York: Ieee.
8. Xie, B. L., & Minn, H. (2012). Real-Time Sleep Apnea Detection by Classifier Combination. [Article]. *Ieee Transactions on Information Technology in Biomedicine, 16*(3), 469-477, doi:10.1109/titb.2012.2188299.
9. Nguyen, H. D., Wilkins, B. A., Cheng, Q., & Benjamin, B. A. (2014). An Online Sleep Apnea Detection Method Based on Recurrence Quantification Analysis. *IEEE Journal of Biomedical and Health Informatics, 18*(4), 1285-1293, doi:10.1109/JBHI.2013.2292928.
10. Lee, H., Park, J., Kim, H., & Lee, K. J. (2016). New Rule-Based Algorithm for Real-Time Detecting Sleep Apnea and Hypopnea Events Using a Nasal Pressure Signal. [Article]. *Journal of Medical Systems, 40*(12), 12, doi:10.1007/s10916-016-0637-8.
11. Berry, R. B., Budhiraja, R., Gottlieb, D. J., Gozal, D., Iber, C., Kapur, V. K., et al. (2012). Rules for Scoring Respiratory Events in Sleep: Update of the 2007 AASM Manual for the Scoring of Sleep and Associated Events. [Article]. *Journal of Clinical Sleep Medicine, 8*(5), 597-619, doi:10.5664/jcsm.2172.
12. Heneghan, C. (2008). ST. Vincent's University Hospital/University College Dublin Sleep Apnea Database. doi:10.13026/C26C7D.
13. Goldberger, A. L., Amaral, L. A. N., Glass, L., Hausdorff, J. M., Ivanov, P. C., Mark, R. G., et al. (2000). PhysioBank, PhysioToolkit, and PhysioNet - Components of a new research resource for complex physiologic signals. *Circulation, 101*(23), E215-E220.
14. Al-Haddad, L., Morris, C. W., & Boddy, L. (2000). Training radial basis function neural networks: effects of training set size and imbalanced training sets. *Journal of Microbiological Methods, 43*(1), 33-44, doi:https://doi.org/10.1016/S0167-7012(00)00202-5.
15. Gutierrez-Tobal, G. C., Hornero, R., Alvarez, D., Marcos, J. V., & del Campo, F. (2012). Linear

and nonlinear analysis of airflow recordings to help in sleep apnoea-hypopnoea syndrome diagnosis. *Physiological Measurement, 33*(7), 1261-1275, doi:10.1088/0967-3334/33/7/1261.

16. Gutierrez-Tobal, G. C., Alvarez, D., Victor Marcos, J., del Campo, F., & Hornero, R. (2013). Pattern recognition in airflow recordings to assist in the sleep apnoea-hypopnoea syndrome diagnosis. *Medical & Biological Engineering & Computing, 51*(12), 1367-1380, doi:10.1007/s11517-013-1109-7.
17. Bloch, K. E. (2003). Getting the most out of nocturnal pulse oximetry. [Editorial Material]. *Chest, 124*(5), 1628-1630, doi:10.1378/chest.124.5.1628.
18. Netzer, N., Eliasson, A. H., Netzer, C., & Kristo, D. A. (2001). Overnight pulse oximetry for sleep-disordered breathing in adults - A review. [Review]. *Chest, 120*(2), 625-633, doi:10.1378/chest.120.2.625.
19. Magalang, U. J., Dmochowski, J., Veeramachaneni, S., Draw, A., Mador, M. J., El-Solh, A., et al. Prediction of the Apnea-Hypopnea Index From Overnight Pulse Oximetry<sup>*</sup>. *Chest, 124*(5), 1694-1701, doi:10.1378/chest.124.5.1694.
20. Olson, L. G., Ambrogetti, A., & Gyulay, S. G. (1999). Prediction of sleep-disordered breathing by unattended overnight oximetry. [Article]. *Journal of Sleep Research, 8*(1), 51-55, doi:10.1046/j.1365-2869.1999.00134.x.
21. Cortes, C., & Vapnik, V. (1995). Support-vector networks. [journal article]. *Machine Learning, 20*(3), 273-297, doi:10.1007/bf00994018.